iJRASET
International Journal For Research in Applied Science and Engineering Technology



INTERNATIONAL JOURNAL FOR RESEARCH

IN APPLIED SCIENCE & ENGINEERING TECHNOLOGY

Volume: 10 **Issue:** V **Month of publication:** May 2022

DOI: https://doi.org/10.22214/ijraset.2022.42914

www.ijraset.com

Call: 08813907089 | E-mail ID: ijraset@gmail.com

International Journal for Research in Applied Science & Engineering Technology (IJRASET)
ISSN: 2321-9653; IC Value: 45.98; SJ Impact Factor: 7.538
Volume 10 Issue V May 2022- Available at www.ijraset.com

Synthesis and Characterization of Silver Doped Zinc Oxide Nanoparticle from Beetle Leaf Extract- Evaluation of Antimicrobial Activity Against Human Pathogenic Bacteria and Fungi

Tanuja[1], Arunkumar Lagashetty[2]
[1]*Phd Student, Department of Nanotechnology Reginal Reserch Center VTU Belagavi, Karntaka India*
[2]*Professor, Dept of Studies in Chemistry Vijayanagar Sri Krishan Devaraya University Ballari*

Abstract: ***Plants or natural resources have been found to be a good alternative method for nanoparticles synthesis. In this study, silver doped zinc oxide nanoparticles (AgZno4NPs) synthesized from* Piper betle *leaves extract were investigated for their antibacterial and antifungal activity. ZnO nanoparticles were prepared from the reduction of Zinc oxide and $NaBH_4$ was used as reducing agent, later doped with silver nitrate. Silver doped zinc nanoparticles were mixed thoroughly and subjected for characterization studies. Prepared nanoparticles were characterized by Visual inspection, Ultraviolet-visible spectroscopy (UV), Fourier transform infrared Spectroscopy (FT-IR), Transmission Electron Microscopy (TEM) techniques. Antimicrobial activities of the synthesized silver nanoparticles were tested against* Staphylococcus aureus *ATCC 25923,* Salmonella typhi *ATCC 14028,* Escherichia coli *ATCC 25922 and* Pseudomonas aeruginosa *ATCC 27853. UV–Vis spectrum of reaction mixture showed strong absorption peak with centering at 400 nm. The FT-IR results imply that Ag-Zn NPs were successfully synthesized and capped with bio-compounds present in* P. betle *and particle size ranging from <100nm. The result revealed that AgZn-Extract NPs showed 12.78±0.64 mm zone of inhibition against* S. typhi*, whereas streptomycin (positive control) showed maximum 15.15±0.40 mm zone of inhibition for* S.mutans*. Again, maximum zone of inhibition found for* S. mutans*. The results obtained by this study can't be directly extrapolated to human; so further studies should be undertaken to established the strong antimicrobial activity of Ag-Extract NPs for drug development program.***

I. INTRODUCTION

Nanotechnology addresses a progressive way for mechanical improvement that concerns the administration of material at the nanometer scale (one billion times less than a meter). Nanotechnology genuinely implies any innovation on the nanoscale that has various applications in reality.

Nanotechnology in a real sense envelops the manufacture and use of substance, physical, and organic frameworks at scales going from individual particles or molecules to submicron aspects, and furthermore the coordination of these subsequent nanomaterials into bigger frameworks. It can possibly alter our points of view and assumptions and furnish us with the ability to determine worldwide issues. Nanotechnology is an emerging field of science which involves synthesis and development of various nanomaterials (Basavaraj et al. 2012). At present, different types of metal nanomaterials are being produced using copper, zinc, titanium, magnesium, gold, alginate and silver. These nanomaterials are used in various fields such as optical devices (Anderson and Moskovits 2006), catalytic (Zhong-jie et al. 2005), bactericidal (Rai and Yadav et al. 2009), electronic (Rao and Kulkarni et al. 2000), sensor technology (Vaseashta et al. 2005), biological labelling (Nicewarner-Pena and Freeman et al. 2001) and treatment of some cancers (Sriram and Manikanth et al. 2010). Currently, there is a growing need to develop environmentally benign nanoparticles that do not use toxic chemicals in the synthesis protocol. As a result, researchers in the field of nanoparticles have turned to biological systems for inspiration. Biosynthetic methods have been investigated as alternatives to chemical and physical ones. The commonest method used to produce silver nanoparticles is chemical synthesis, employing reagents whose function is to reduce the silver ions and stabilize the nanoparticles. These reagents are toxic and can present risks to health and the environment (Ahmed et al., 2016; Zhang et al., 2016), which has led to increasing interest in biogenic synthesis methods. Such processes enable nanoparticles to be obtained that present lower toxicity, better physicochemical characteristics, and higher stability (Iravani et al., 2014).

©IJRASET: All Rights are Reserved

Biogenic synthesis of nanoparticles can be performed using organisms such as bacteria, fungi, and plants, or the byproducts of their metabolism, which act as reducing and stabilizing agents (Durán et al., 2011). These nanoparticles are capped with biomolecules derived from the organism used in the synthesis, which can improve stability and may present biological activity (Ballotin et al., 2016). Biogenic synthesis is relatively simple, clean, sustainable, and economical, and provides greater biocompatibility in the uses of nanoparticles (Gholami-Shabani et al., 2014).

A. Biological Applications of Nanoparticles

Tissue designing: Titanium is a notable bone fixing material generally utilized in muscular health and dentistry. It has a high crack opposition, flexibility and weight to strength proportion. Tragically, it experiences the absence of bioactivity, as it doesn't uphold sell grip and development well. Apatite coatings are known to be bioactive and to cling deep down. Henceforth, a few methods were utilized in the past to deliver an apatite covering on titanium.

Those coatings experience the ill effects of thickness non-consistency, unfortunate grip and low mechanical strength. Furthermore, a stable permeable design is expected to help the supplements transport through the cell development. It was shown that utilizing a biomimetic approach - a sluggish development of nanostructured apatite film from the reproduced body liquid - brought about the arrangement of a firmly follower, uniform nanoporous layer. The layer was viewed as worked of 60 nm crystallites, and have a stable nanoporous construction and bioactivity.

Cancer Therapy: Nanoparticles may activate innate and/or adaptive immune systems and trigger anti-cancer immune response. Furthermore, targeting cancer stem-like cells by nanoparticles helps eliminate drug resistance and tumor recurrence, or prevent metastasis. Mejorly gold and silver nanaoparticles were using for cancer therapy due to their less toxic effects on the cells.

Protein detector: Proteins are the important part of the cell's language, machinery and structure, and understanding their functionalities is extremely important for further progress in human wellbeing. Gold nanoparticles are widely used in immunohistochemistry to identify protein-protein interaction. However, the multiple simultaneous detection capabilities of this technique are fairly limited. Surface-enhanced Raman scattering spectroscopy is a well-established technique for detection and identification of single dye molecules.

Nanotechnology involving synthesis and applications of nanomaterials is a rapidly growing field with significant applications in various areas (Duran et al. 2005). The attraction of silver nanoparticles (AgNPs) is mainly because of its application in therapeutics, biomolecular detection, catalysis and also as antimicrobial agents (Sadhasivam et al. 2010; Shrivastava et al. 2009; Wei et al. 2008; Christopher et al. 2011). Microbial synthesis of nanoparticles is eco-friendly and has significant advantages over other processes since it takes place at relatively ambient temperature and pressure (Gade et al. 2008; Mukherjee et al. 2008; Wei et al. 2012). As the size and shape of nanoparticles can also be controlled in microbial synthesis (Narayanan and Sakthivel 2010), screening of unexplored microorganisms for AgNPs synthesizing property is very important.

II. MATERIALS AND METHODS

A. Material used

Silver nitrate from Himedia, Ferric chloride, SRL life sciences, ammonium hydroxide, SRL life sciences, beetle leaves hydroalcoholic extract.

1) *Collection and Preparation of plant Material:* Piper beetle (Beetal leaves) were collected in the season of September-october in the region of Kodagu, Karnataka, India. Leaves were thoroughly washed with tap water fallowed by distilled water to remove the impurities. Later leaves were shade dried under sunlight for 5 days and subjected to the hydro alcoholic (70:30) extraction using Soxhlet apparatus.
2) *Preparation of* AgZnO4 *nanoparticles from beetal leaves extract:* In a clean 250ml glass beaker, 0.649 g of Zink chloride was dissolved in 100ml of double distilled water, and keep it in the stirrer for complete solubility. Meanwhile, weight, 0.1M, 0.286g of silver nitrate and added to the above solution under dark condition and continue the stirring. Set the pH of the solution to 10.5 using NH4OH solution, later add the 1ml of the plant extract in to it and allow to stir on magnetic stirrer at 60^{o}C for 2hr.When a solution get precipitated, stop the stirrer and allow to settle down in room temperature. Precipitated solutions were transferred to the centrifuge tubes and centrifuge at 10000 rpm for 10min, remove the supernatant and continue the centrifugation steps with water fallowed by ehanol for thrice. Then dry the pellet using hot air over for 6hr at 40oC and store the synthesized nanoparticles in airtight box.

$$2Fe(cl_3) + 2AgCl_2 + 8NaoH \rightarrow AgFeO_4 + Fe(OH)_3 + Ag(OH_2) + 8Nacl_2$$

B. Characterization of AgZnO4 Nanoparticles

1) *UV-Visible Spectroscopy:* The reduction from Ag^{+} to Ag^{O} after adding 1mM $AgNo_3$ solution to zinc solution and beetle leaf extracts for the synthesis of BT *–AgZnO4NPs* was monitored using UV visible spectral analysis (Beckman-Coulter DU-730 UV-Vis Spectrophotometer, USA) with wave length (λ) scan from 200 to 800nm in different time intervals. (Surendra make 3 waves in UV, one for Ag, one for Zn and one for beetle leaves)
2) *Dynamic Light Scattering analysis(DLS):* Particle size and zeta potential Distribution of synthesized BT *–AgZnO4NPs* was analyzed by performing DLS (Microtrac- DLS, W3231). The powder sample of the synthesized metal oxide nanoparticles were completely dispersed in water by placed in a zeta chamber analyzing size and zeta potential in different ports. The crystal structure identification confirmation for synthesized BT *–AgZnO4NPs* was done by powder XRD (RIGAKU X-ray diffractometer, model-smart lab 3kw with cu Kα source at 2θ angle probed 10^0-80^0). Fine powder of BT *–AgZnO4NPs* was placed in a platen in different time points and scanned to detect the width of XRD peaks at a rate of 3^o/min and average size of the LR *–AgZnO4NPs* was estimated using De-Broglie Equation ($n\lambda = 2d\sin\Theta$).
3) *SEM and EDS analysis:* The powder sample of BT *–AgZnO4NPs* was placed in different port on carbon coated plate of the scanning electron microscopy, the plate was gold coated by spatter-coater gold coating instrument to increase the conductivity and give fine picture. Imaging was performed to analyze morphological structure and shape of produced BT *–AgZnO4NPs* using Scanning electron microscope (Hitachi, S-3400N, Japan).By using this analysis to identify the crystalline nature of BT *–AgZnO4NPs* and also observe the optical absorption peak from the surface plasma response, by the EDS (Thermo fisher scientific, Noran System 7, USA) analysis for identifying other elemental O, Cl signals are recorded to detect enzymes and other proteins present in synthesized BT *–AgZnO4NPs*.

C. Determination of antimicrobial activity of AgFe2O4NPs *from leaves extract of L. reticulata*

1) Antibacterial Activity

The synthesized *$AgFe_2O_4NPs$* facilitated from beetle leaves were screened for antibacterial against Gram-positive (*S.Mutans* MTCC 7443) and Gram negative (*Salmonella Typhi/*MTCC 3858) and Candida albicans as a fungi, laterally with streptomycin were carried out by well diffusion method [24]. Test bacteria and fungi were seeded evenly onto the surface of nutrient agar (NA) media maintaining a concentration of 1.5 x 10^8 CFU mL^{-1}using a sterile glass spreader. The sterile discs (6 mm) were loaded with 50 µL of *piper betle* (dispersed in sterile distilled water) and placed on agar plates along with standard streptomycin. The inoculated plates were incubated for 24 h at 37 ± 2° C and the zone of inhibition were measured around the discs. The experiment was repeated in triplicates along with standard.

2) Minimum inhibitory concentration determination of Zn –AgZnO4NPs against human pathogens

The minimum inhibitory concentrations (MICs) of synthesized BT–*AgZnO4NPs* nanoparticles were evaluated against human pathogenic bacteria by broth microdilution method described by Agyare et al with little modifications using 96-well microtiter plate. Firstly 100 μL double strength nutrient broth was added each well and 50 μL of different concentration of Ag nanoparticles within the range of 2 to 15mM were

Prepared and 20 μL of 1×10^6CFU/mL inoculum was added to each wells. The plate was incubated at 37∘C for 24 h. 0.1% 20 μL of Resazurin was added to each well after incubation and again plate was incubated at 37◦C for 4 h. The bacterial growth was observed as purple coloration, while clear/yellow coloration indicated no growth. The lowest concentration which showed no visible growth upon the addition of resazurin was considered as MIC value. Streptomycin at concentration ranging from1.0 to 10.0 μg/mL was used as reference standards. The procedure was performed in triplicates.

3) Determination of cellular Protein Leakage Assay

(Joshi A *et al.* 2020) Protein leakage assay was done to analyze the bacteria cell killing potency of the synthesized nanoparticles by estimating the protein content by lowrys method.

Test organism: *S.typhi* , *S.mutant* and *C.albicans* were used.

Sample preparation: various concentration of silver nanoparticles (1×MIC, 2×MIC).

S.typhi	S.mutant	Candida albicans
(1×6.25,2×6.25)ENPS	(1×6.25, 2×6.25) ENPS	(1×25, 2×25) ENPS
(1×3.125, 2×3.125)LNPS	(1×6.25, 2×6.25)LNPS	(1×50,1×50) LNPS

Method

- Cells are grown to a final density of 1.5×10^5 CFU/ml were incubated into LB media.
- Various concentration of siver nanoparticles (1×MIC, 2×MIC) , of concentration of *S.typhi, S,mutant* and *C.albicans.*
- In control no AgNPSs were added only inoculum was incubated at 37^oc for 24 hrs.

1ml of each culture was centrifuge at 3000 rpm for 10 min then collect the supernantant which contains the protein leaked from the dead microbial cells and estimated the protein content using lowry'smethod.

D. Estimation of protein by lowrys method: (LOWRY OH et al.1951)

Reagents : solution A- sodium carbonate, 0.1N NaOH, Solution B -0.5% copper sulphate, 1% sodium potassium tartrate . Lowrys reagent- solution A and solution B were mixed.

Method

- Working standard of 0.2- 1mg/ ml of BSA was pipetted out into clean test tube labelled as S1-S5.
- Different concentration of AgZnO4NP's were added and add distilled water make up to 1ml distilled water take as blank.
- 3ml of lowry's reagent was added to all test tube.
- Followed by 0.5 ml of FC reagent was added then incubate in a room temperature for 30 minutes.
- After Incubation measure the OD at 660nm using spectrometer.

III. RESULTS AND ANALYSIS

A. UV Visible Spectrometer

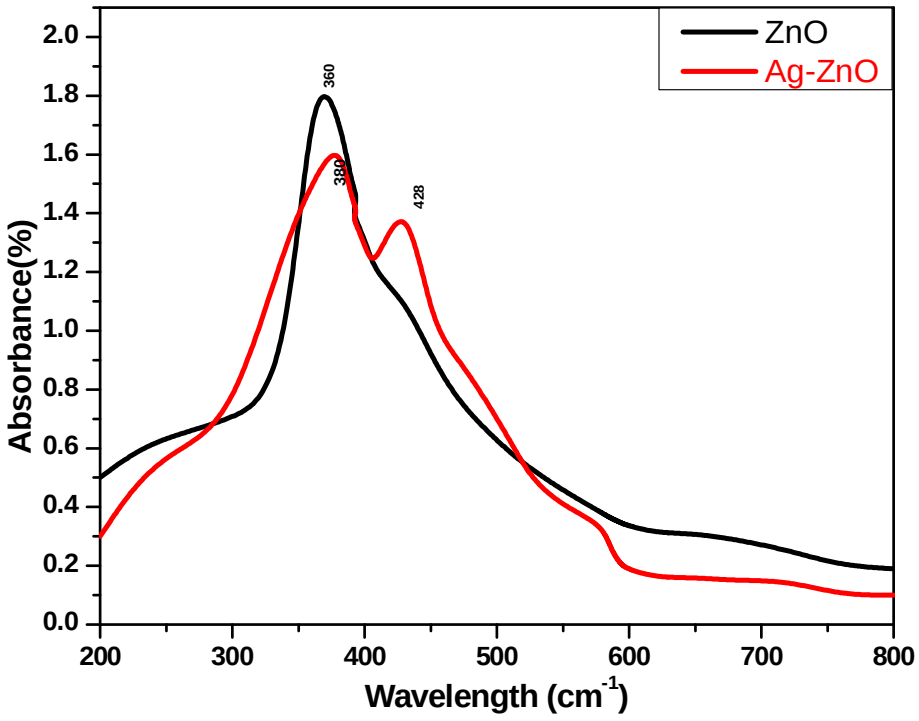


Fig:1: UV -visible spectroscopy of Zno and Ag doped Zno nanoparticles

Electronic absorption or UV-visible spectroscopy is one of the simplest and yet most useful optical techniques for studying optical and electronic properties of nanomaterials. The UV-visible spectra for BT- AgZnO nanoparticles, have been recorded in the range 360-428 nm **(Fig 1). The absorption peaks for nanoparticles were shows at 360, 380 and 428 nm correspond to $\pi\rightarrow\pi^*$ and $n\rightarrow\pi^*$ transitions for Zno, Ag-Zno and plant extract respectively.** This clearly indicates that ZnNPs conjugates with Ag metal oxide and beetle plant extract. The results from UV-vis parallel with that from XRD, and IR spectra, for same conjugation.

B. XRD Analysis of BT- AgZnO Nanoparticles

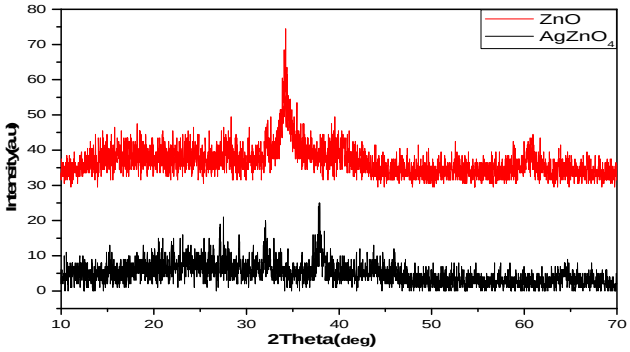


Fig:2: XRD analysis of Zno and Ag doped Zno nanoparticles

The crystalline nature of the AgZnONPs was evaluated by X-ray diffraction (XRD) technique, it is used to calculate average size, Bravais lattice and intensity of nanoparticles. The XRD pattern of NPs, is shown in Fig. 2. The crystallinity of the BT-AgZnONPs revealed by the presence sharp peaks in the XRD pattern. The diffractogram of nanoparticles showed well resolved four diffraction peaks at 2θ angles of 35.32°, 38.83°, which corresponds to the braggs reflection peaks of (70), (68) and (80) planes of face centered cubic (fcc) structures.

However in the XRD of AgZnONPs-linker-plant extract, it is observed second and fourth peaks at 2θ values in the range of 1.8 and 1.4 and with average crystallite size in between 236.38-433.15 nm. By comparing the XRD of ZnNPs-linker-drug with that of AgNPs and BT leaf extract, it is clear that, the XRD of AgNPs-linker-plant extract contains all the peaks that correspond to AgZnoNPs and BT extract. This interaction is again confirmed by change in intensity of the peak and also band broadening.

C. FTIR Analysis of BT-AgZnO Nanoparticles

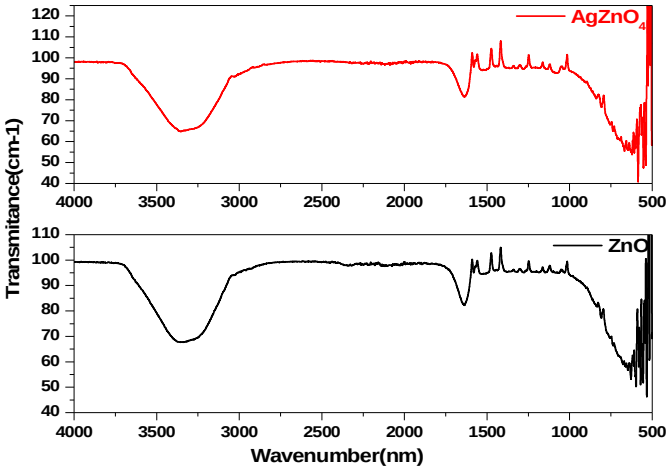


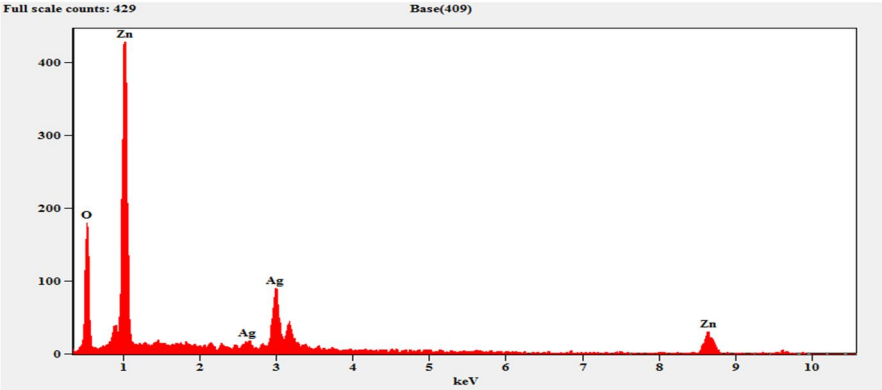
Fig:3: FTIR analysis of Zno and Ag doped Zno nanoparticles infused with beetle leaf extract

The FT-IR spectroscopic analysis was performed to surmise the information on the probable biomolecules of BT liable for the integration of BT-AgZnONPs represented as Fig.4A sequentially. The analysis of the FT-IR spectrum of plant extracts of BT leaves and Zinc doped silver nanoparticles were characterized by the sharp peak observed at 3400 cm-1 strong OH bond 2070 cm-1 CN THRIPLE BOND 1 , and 1610 cm^{-1}, 1520 cm^{-1} which corresponds to carbonyl stretching frequency and 1394 cm^{-1} 993 cm^{-1} 699 cm^{-1} 628 cm^{-1} CH phase bending individually. The metal-oxygen bonding and nature of the synthesized oxide sample was carried out by infrared study. Metal oxides generally give absorption bands below 1000 cm1 arising from inter-atomic vibrations [19]. The peak 3325 cm1 corresponds to water of absorption. Vibrational frequency at 1610 and 1520 cm1 is due to the presence of carbon dioxide. Peaks below 1000 cm1 corresponds to Metal-oxygen (M-O) vibrational modes of the samples conform the formation of Ag doping Zinc.

©IJRASET: All Rights are Reserved | SJ Impact Factor 7.538 | ISRA Journal Impact Factor 7.894 |

D. EDX and SEM analysis of BT-AgZnONPs

To know the presence of silver in the synthesized silver nanoparticle doped with zincoxide and size of the synthesized particles, the analysis of the sample was performed by EDX technique. The figure-5 shows EDX spectrum of as synthesized silver nanoparticles. This spectrum shows the presence of strong silver atom and Zinc atom signal and a characteristic absorption peak of silver confirms the formation of silver nanoparticles. The synthesized nanoparticle showed 100nm in size with confirming the presence of zinc and silver ions.



Element Line	Weight %	Weight % Error	Atom %
O K	23.30	± 3.30	59.57
Zn K	46.07	± 5.83	28.82
Zn L	---	---	---
Ag L	30.63	± 2.46	11.61
Ag M	---	---	---
Total	100.00		100.00



Fig:3: EDX and SEM analysis of BT-AgZnONPs

The morphology of the as prepared BT-AgZnONPs nanoparticles was studied by scanning electron micrograph image tool. Figure-5C shows SEM image of as prepared AgZno nanoparticle sample. This image shows, the most of the particles are spherical in nature with close compact arrangement, and rod-shaped zinc oxide element. In addition to this particle agglomeration with semicrystalline nature.

©IJRASET: All Rights are Reserved | SJ Impact Factor 7.538 | ISRA Journal Impact Factor 7.894 |

E. Evaluation of antibacterial activity of the silver nanoparticles synthesized by bacterial biomass.

Minimum Inhibitory concentration determination against S***.typhi (Salmonella typhi)***

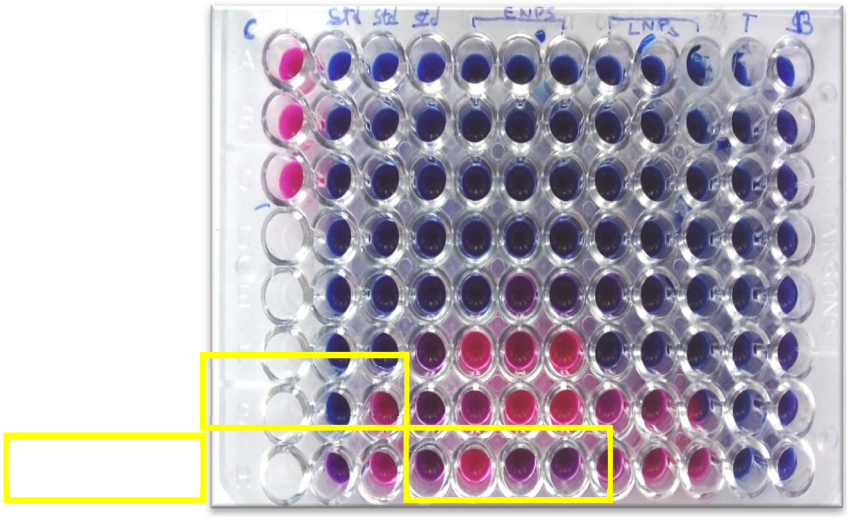


Figure:4: Minimum inhibitory concentration estimation against *S.typhi*

F. Graphical Representation of MIC

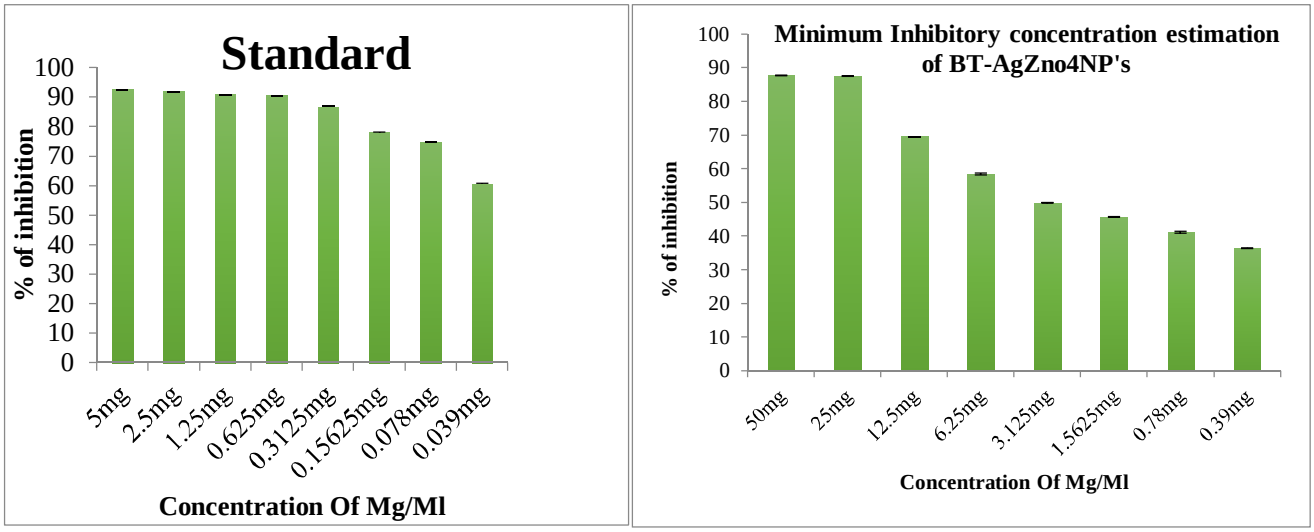
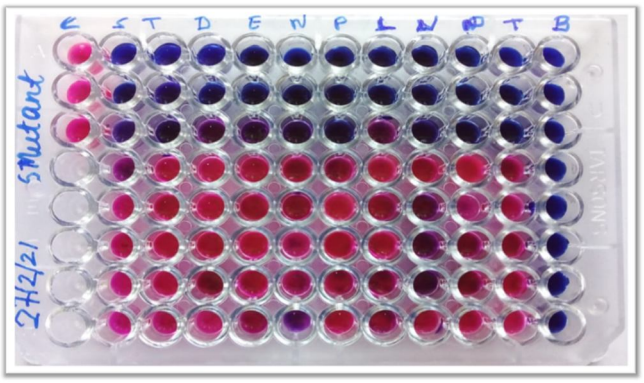


Figure:4: Showing 96 well plate with the resazurin dye inhibition (A), Standard streptomycin showing inhibition activity against *S.typhi* (B), NP's showed the dose dependent inhibitory activity against S. typhi. (C&D)

Microdilution and agar dilution are the two quantitative methods to determine the MIC values of the compounds (Kim et al. 2007). While results obtained with the agar dilution method show good correlation with the microdilution method but (Amsler et al. 2010), the agar dilution method is laborious, time consuming and more importantly the factors that adversely affect the disc diffusion method may also contribute to the lack of accuracy with the agar dilution method especially when dealing with partially soluble compounds. The improved microdilution method defined in this study is enhanced through the addition of resazurin dye as a redox indicator, which overcomes the problems associated with sparingly soluble test materials. Active bacterial cells reduce the non-fluorescent resazurin (blue) to the fluorescent resorufin (pink) which can be further reduced to hydroresorufin (O'Brien et al. 2000) as shown in Fig. 4 giving a direct quantifiable measure of bacterial metabolic activity. Minimum inhibitory concentration of AgZnNP's were estimated using resazurin method. For standard, (5mg/ml) streptomycin is used and it showed the MIC concentration at 0.15mg/ml. NP's showed MIC at 3.125mg/ml ZnNP's showed the dose dependent inhibitory activity against *S. typhi*.

ISSN: 2321-9653; IC Value: 45.98; SJ Impact Factor: 7.538
Volume 10 Issue V May 2022- Available at www.ijraset.com

G. Minimum inhibitory concentration estimation of BT-AgZnO4BT-AgZnO4NP's against S. Mutans



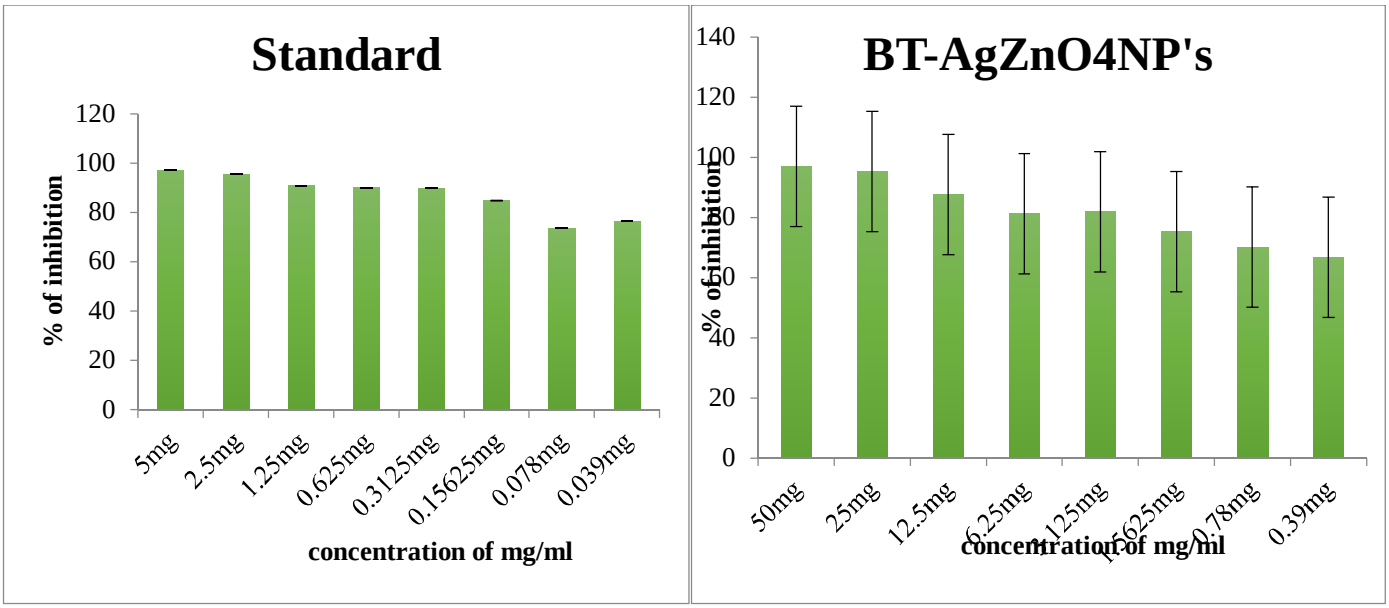
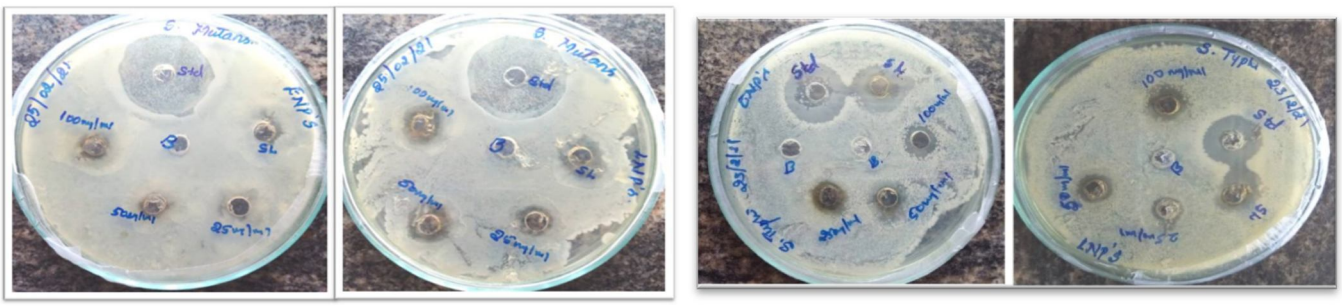


Figure:5: Showing 96 well plate with the resazurin dye inhibition, Pink colour indicates the bacterial growth and blue colour indicates inhibition (A), Standard streptomycin showing inhibition activity against *S. Mutans* (B) NP;s showed the dose dependent inhibitory activity against S. typhi. (C&D)

Minimum inhibitory concentration of NP's were estimated using resazurin method. For standard, (5mg/ml) streptomycin is used and it showed the MIC concentration at 1.25mg/ml. NP's showed MIC at 12.5 mg/ml against S. Mutans. S. Mutans is a gram positive bacterial commonly found in human oral cavity and cause the decaying of the tooth. Synthesized silver nanoparticles using lactobacillus (BT-AgZnO4NP's) and E.coli (AgZnO4NP's) showed the great inhibiting activity against S. typhi, as well, they showed inhibiting activity against S. mutans at highest concentration when compared to S. typhi. Therefore, synthesized nanoparticles having great inhibiting ability against gram negative bacterial which are more pathogenic compared to gram positive.
Evaluation of antibacterial activity of the BT-AgZnO4NP's against *S.Typhi* and *S. Mutans*



©IJRASET: All Rights are Reserved

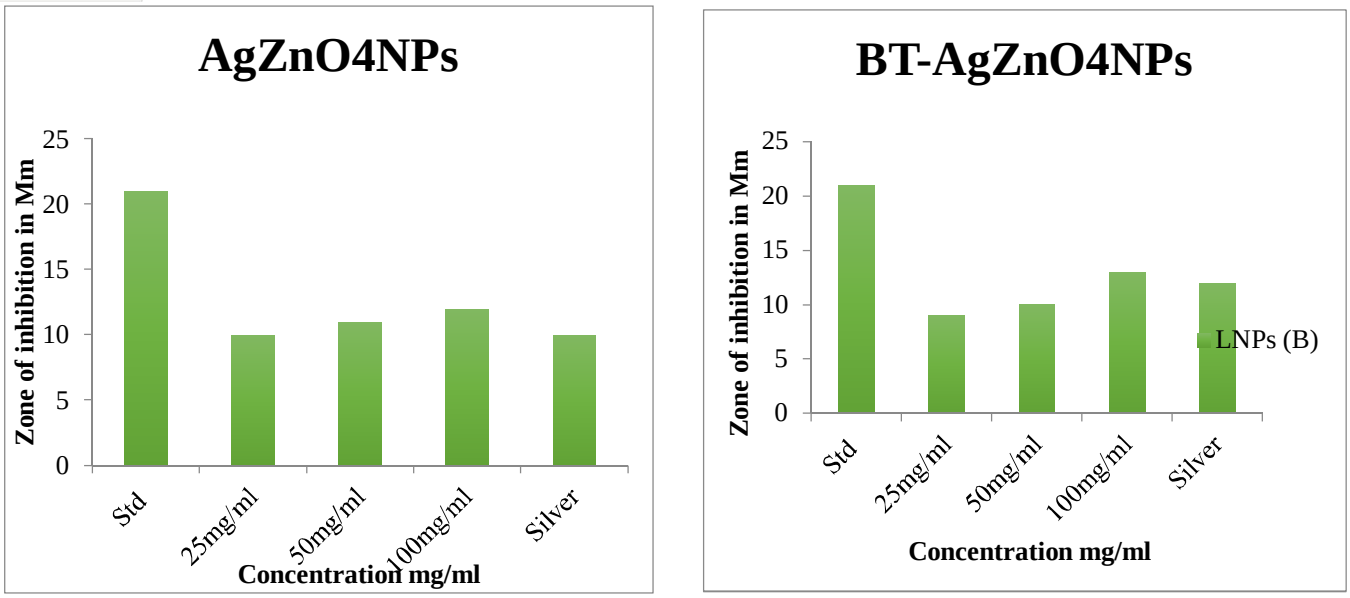
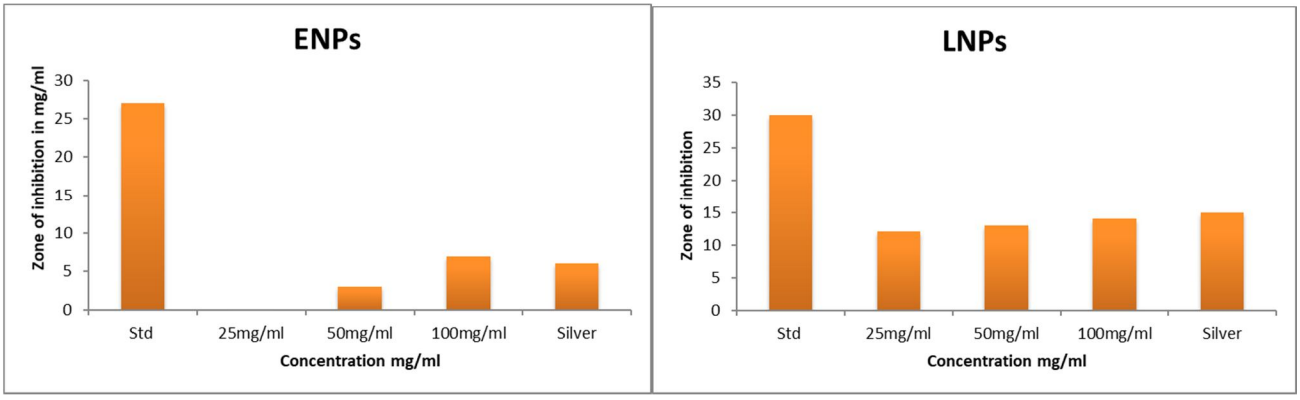


Figure 6: Showing antibacterial activity of the AgZnO4NP's and BT-AgZnO4NP's by agar well cup method.(A). Graphical representation of the AgZnO4NP's and BT-AgZnO4NP's against *S. Typhi* and *S. Mutans* (B)

H. S. Typhi



I. S. Mutans

Table: 1: Showing Zone of inhibition of AgZnO4NP's and BT-AgZnO4NP's against S. Typhi and S. Mutans

Zone of inhibition in Mm						
Organism: *Salmonella Typhi*						
Test Compounds	Std	Blank	25mg/ml	50mg/ml	100mg/ml	Silver
AgZnNPs (A)	21 Mm	…	10Mm	11Mm	12Mm	10Mm
BT-AgZnNPs (B)	21Mm	…	9Mm	10Mm	13Mm	13Mm
Organism: *streptococcus mutants*						
AgZnO4NPs (A)	27 Mm	…	0Mm	3Mm	7Mm	6Mm
BT-AgZnO4NPs (B)	30Mm	…	12Mm	13Mm	14Mm	15Mm

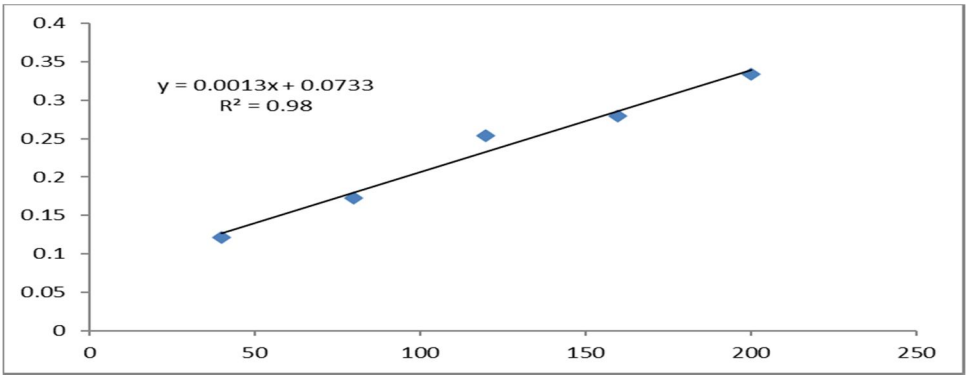
©IJRASET: All Rights are Reserved | SJ Impact Factor 7.538 | ISRA Journal Impact Factor 7.894 |

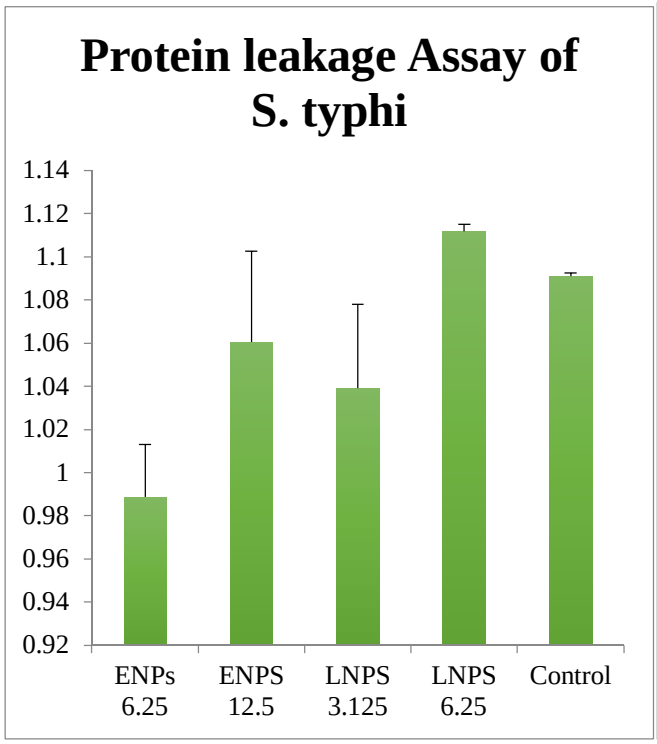
Subsequently, once the MIC concentration of the silver nanoparticle found out, 3 highest concentration above the MIC were selected for the agar well diffusion method. As well can observe in the Figure( ), 50mg/ml and 100mg/ml concentration of the both BT-AgZnO4NP's and AgZnO4NP's showed the better activity. This result is corelate with the MIC assat that, compounds showed the highest inhibition against gram negative bacterial *S. typhi* compared to *S. Mutans* (table:1)

Silver nanoparticles interferes with bacterial growth signaling pathway of alleged peptides substrate which is important for cell viability and division. The Gram stain Catalase Coagulate Oxidase Motility salmonella typhi Positive + & *Strptococcus mutans* Negative +. The major mechanism over silver nanoparticles demonstrated antibacterial properties was by attaching to and piercing the bacterial cell wall, and controlling cellular signaling by dephosphorylating putative key peptide substrates on tyrosine residues (Shrivastava et al., 2007). The nanoparticles show inimitable biological and chemical properties which make them excellent agents for many purposes in the medical and pharmaceutical field (Jain and Aggarwal, 2012). The result of current work indicates that the synthesized Ag nanoparticles from bacterial reduction process have antibacterial properties. When the Ag-nanoparticles were tested on salmonella typhi and*s mutans*, the zones of inhibition were obtained in both the bacteria. These differences in the zones of inhibition may be directly related to the susceptibility of each test organisms to the Ag nanoparticles.

J. Protein Leakage Assay of AgZnO4NP's and BT-AgZnO4NP's against S. typhi and S. Mutans

Standard Graph of Bovine serum albumin





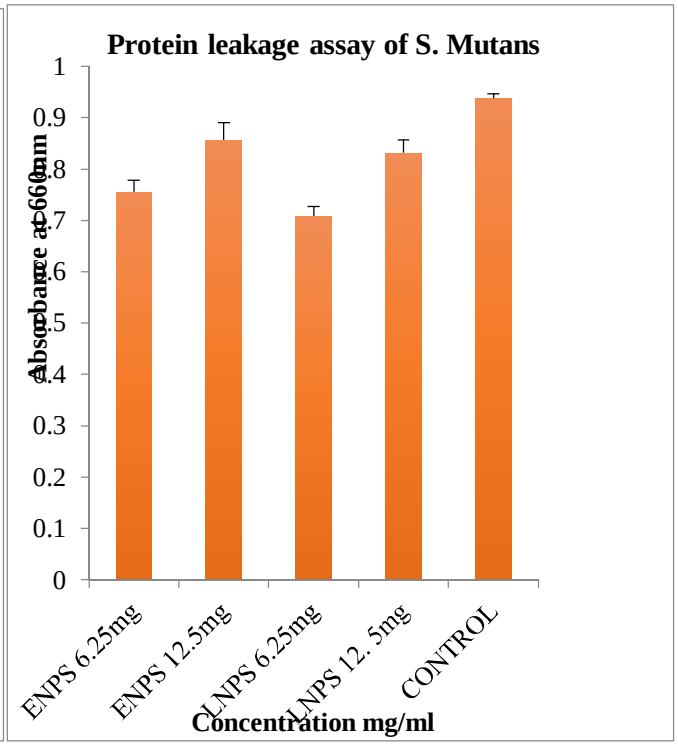


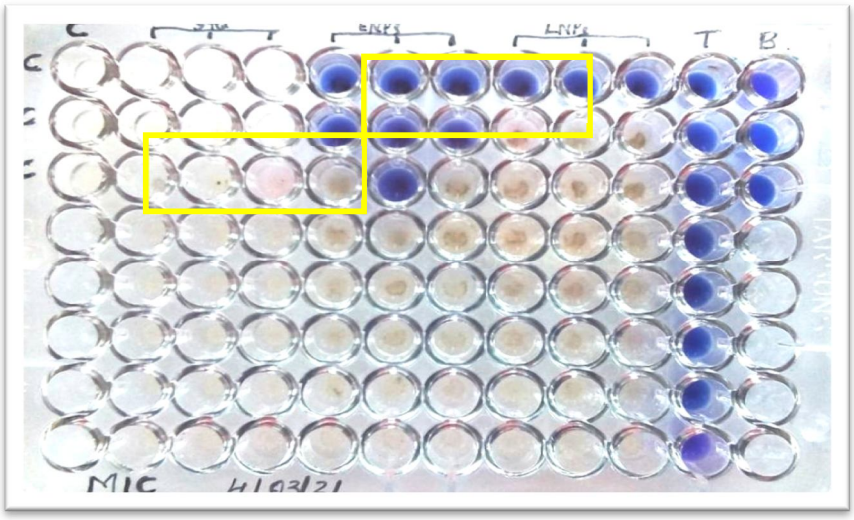
Figure :7: Data showing cell wall protein leakage assay of the AgZnO4NP's and BT-AgZnO4NP's. A) Standard BSA graph, B) Protein leakage content from S. typhi biomass and C) protein leakage from *S. Mutans* biomass.

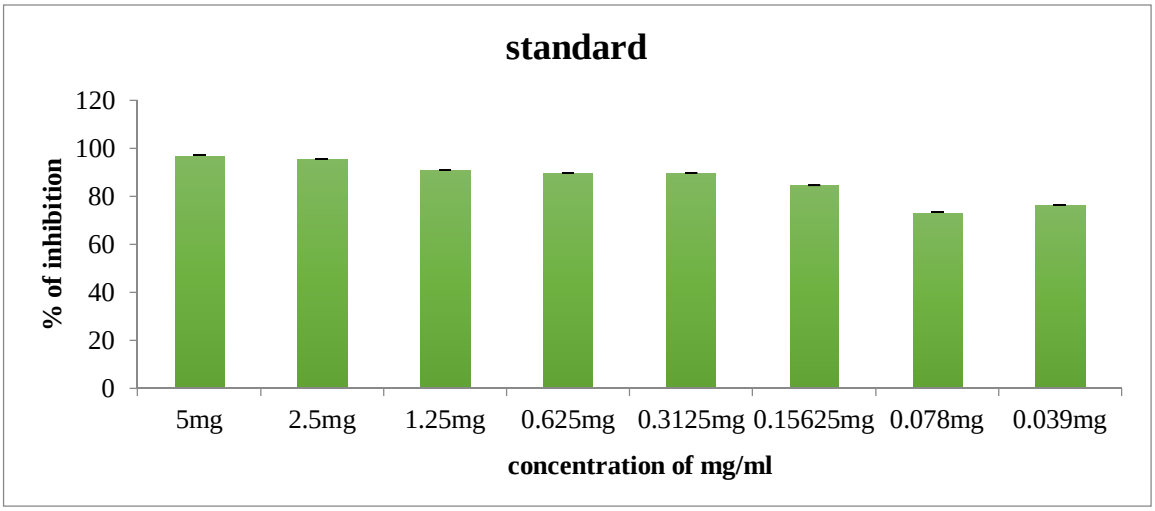
To confirm the effects of Silver nanoparticles synthesized from bacterial reduction (AgZnO4NP's and BT-AgZnO4NP's) on metabolic activity, we analyzed the levels of intracellular macromolecules such as proteins. Previous studies have confirmed that AgNPs cause protein leakage by increasing membrane permeability in bacteria (Gurunathan, 2014). Therefore, we determined the effect of AgZnO4NP's and BT-AgZnO4NP's on protein leakage by treating *S. typhi* and *S. Mutans* cells with AgNPs at their MIC (1×MIC and 2×MIC and 3×MIC mg/ mL, respectively) for 24 h to further provide the conformation for the antibacterial activity. The amounts of protein released in the suspension of the treated cells were estimated using the lowries method. Protein leakage was found to be higher in silver nanoparticle-treated cells compared to untreated cells, especially BT-AgZnO4NP's treated group compared to AgZnO4NP's (Figure.7).

However, BT-AgZnO4NP's -treated S. typhi showed significantly higher protein leakage (1.1 mg/ml) compared to *S. mutans* cells (125 µg/mg), suggesting that the gram-positive S. mutans had lower antibacterial sensitivity than that of the gram-negative S. typhi . Similarly, **Soo-Hwan et al.** found that protein leakage was significantly higher in E. coli than S. aureus. **Gurunathan et al.** showed that protein leakage was significantly higher in the gram-negative bacteria Escherichia fergusoni compared to the gram-positive Streptococcus mutans. The observed changes in protein leakage could be due to the differences in the structural features of the cell wall, particularly the thickness of the peptidoglycan layer, which functions as a protective barrier against antibacterial agents, such as antibiotics, toxins, chemicals, and degradation enzymes. Altogether, our results were consistent with those of previous studies showing that silver nanoparticles disrupt the bacterial membranes, consequently leading to intracellular leakage of macromolecules. found to be higher in AgNP-treated cells compared to untreated control cells (Figure).

K. Evaluation of anti-fungal activity of silver nanoparticles against Candida albicans

1) Minimum Inhibitory Concentration Assay





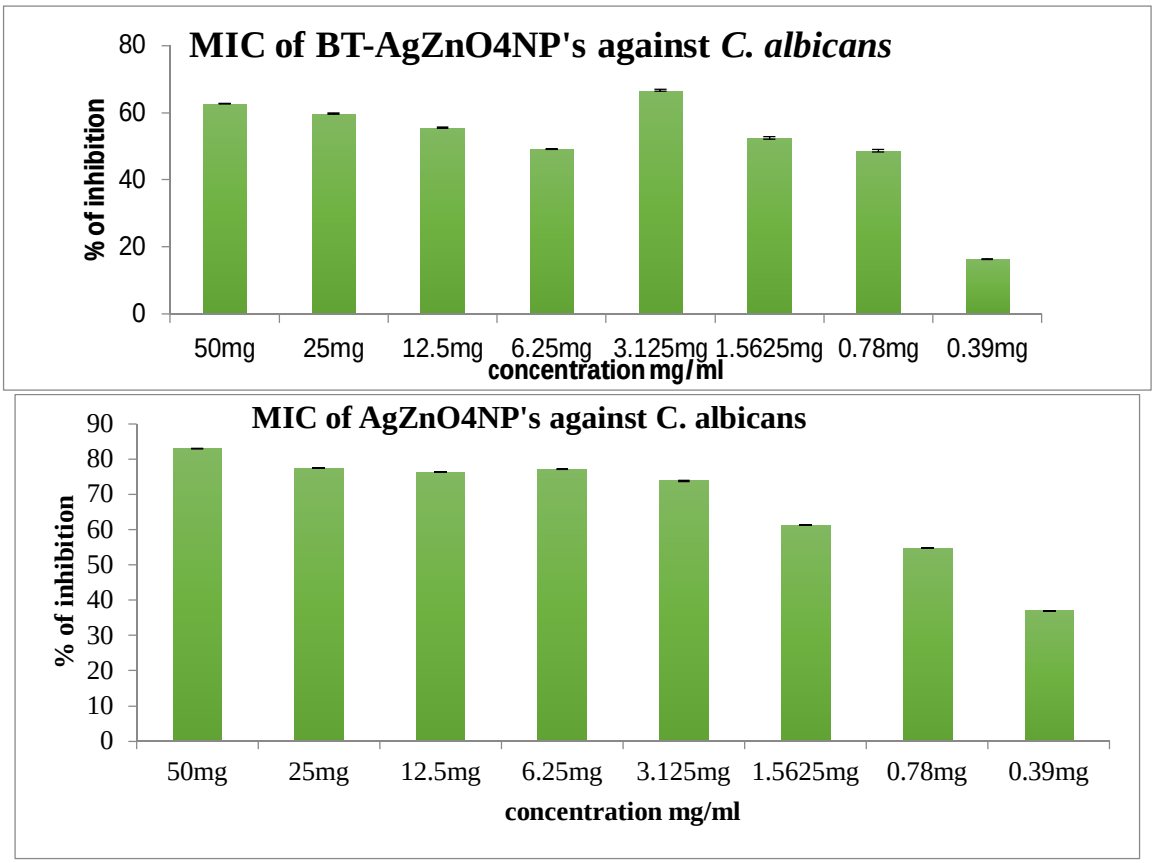


Figure:8: Showing Minimum inhibitory concentration estimation of BT-AgZnO4NP's and AgZnO4NP's against C. albicans by rezasurin method (A), Graphical presentation of Standard Clotrimazole MIC against C. albicans (B), Graphical representation of the % of inhibition of AgZnO4NP's and BT-AgZnO4NP's silver nanoparticles against c. albicans.

Minimum inhibitory concentration of the synthesized nanoparticle were analyzed by rezasurin dye reduction method (A), clotrimozole used as standard(B), Graph showing AgZnO4NP's and BT-AgZnO4NP's (C&D). Standard Drug didn't showed effective inhibitory activity against C. albicans, whereas, AgZnO4NP's showed 25mg/ml as a MIC and BT-AgZnO4NP's showed 50mg/ml as a MIC value to inhibit the C. albicans growth.

Antibacterial activity of the synthesized nanoparticles by Zone inhibition method

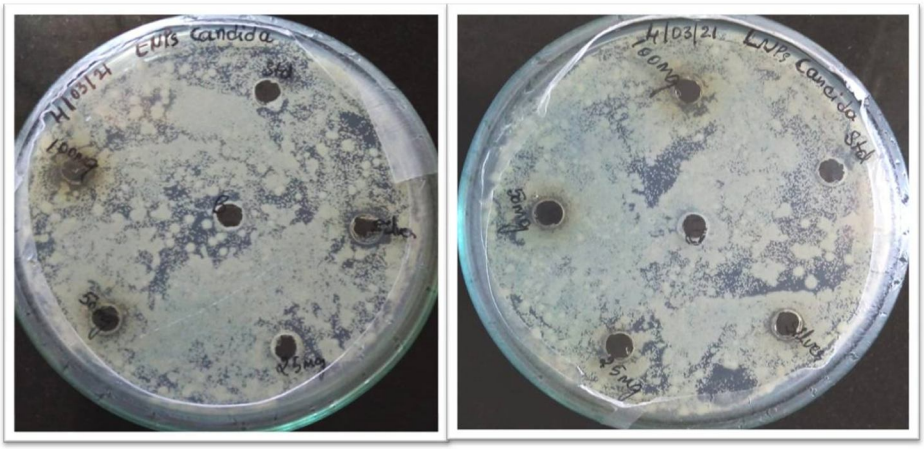


Figure: 09: Zone of inhibition of the synthesized nanoparticles against *C. albicans* by agar well method.

©IJRASET: All Rights are Reserved | SJ Impact Factor 7.538 | ISRA Journal Impact Factor 7.894 |

In the agar well diffusion method, the wells were loaded with various concentrations of synthesized silver nanoparticles (25,50 & 100mg/ml) showed slight to moderate inhibition of fungal growth by forming a crescent shaped inhibition zone around discs incorporated with nanoparticles. There was no significant result observed in inhibiting the C. albicans, There were slight inhibition found in 100mg/ml treated NP"s groups compared to BT-AgZnO4NP's. Standard positive drug also did n't showed any significant result.

L. Cell wall Protein Leakage Assay

BSA standard Graph

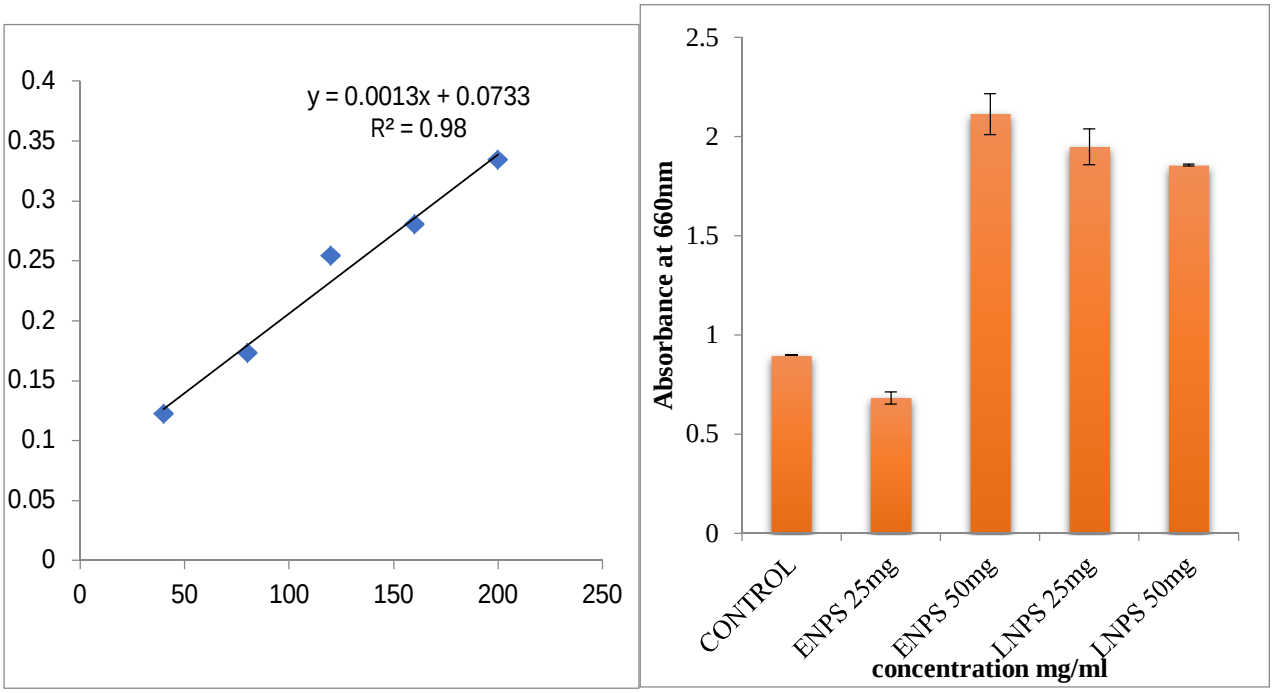


Figure :10: Protein leakage assay by lowries method. Standard BSA graph (A), effect of AgZnO4NP's and BT-AgZnO4NP's on protein leakage from the fungi biomass (B)

Size is said to have an influence on the silver nanoparticle's mechanism to enter the cell membrane leading to its death [65]. Cells of *C. albicans* experienced a huge leakage of proteins after incubation with different concentrations of silver doped zinc beetle leaf nanoparticles (Fig. 11). It was also observed that there was an increase in protein leakage as the concentration of nanoparticles increased. Similar results were described by Ghosh and Ramamoorthy [68]. Twenty nanograms per milliliter of silver nanoparticles has made E. coli and Enterobacter sp. to leak protein [39].

IV. CONCLUSION

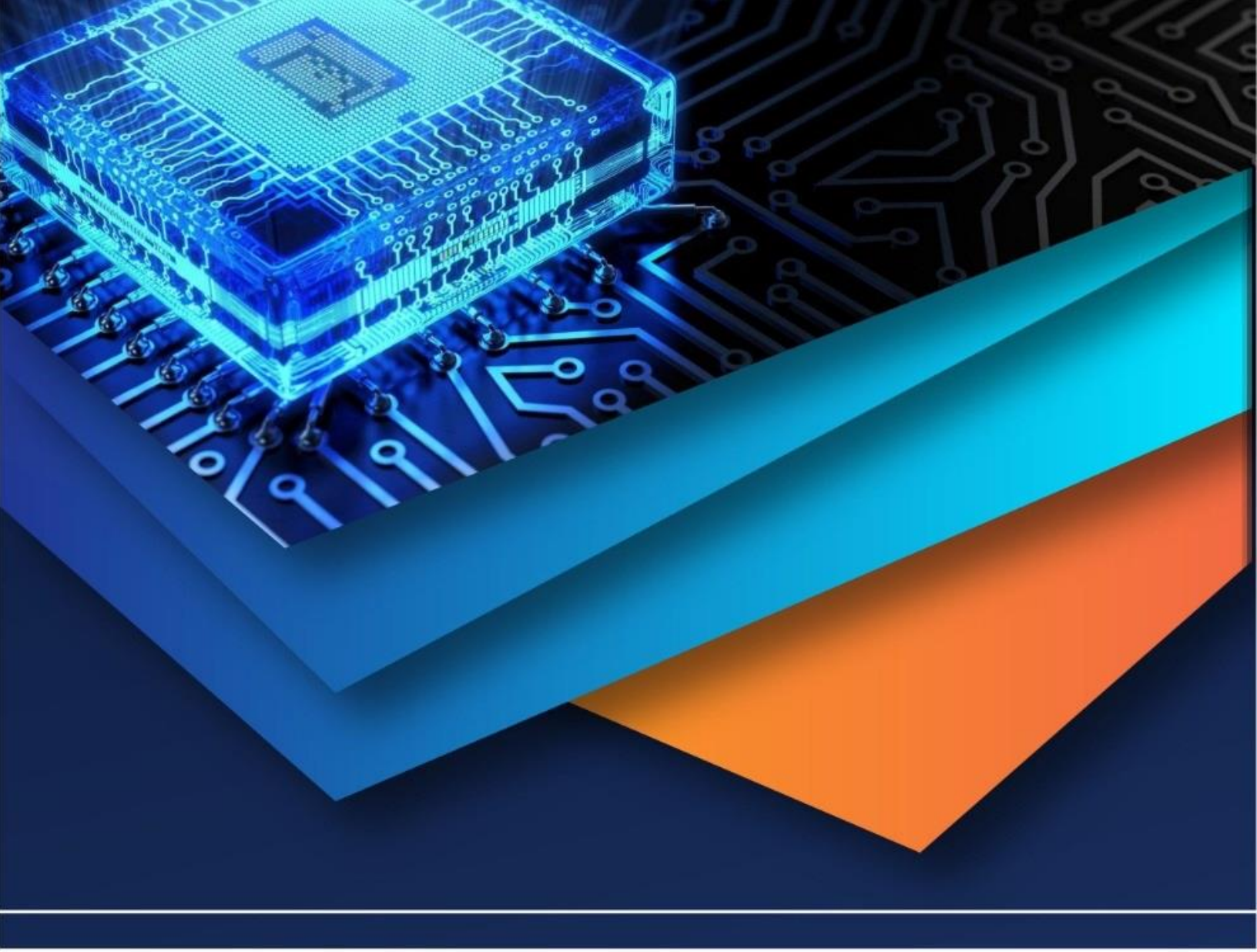
The biosynthesis of nanoparticles using bacterial cells are eco-friendly, easy to synthesize and exhibit the broad spectrum of biocidal activity toward several types of bacteria and fungi. In the synthesized silver nanoparticles from lactobacillus and E. coli FTIR spectroscopy revealed the involvement of functional groups in the bio reduction of Ag+ to Ag0 and UV-vis spectra exhibit the peak at 406 nm characteristics of AgNPs. Both AgZnO4NP's and BT-AgZnO4NP's Ag nanoparticles were able to inhibit the growth of *salmonella typhi* and *S. Mutans* bacteria by damaging the bacterial cell wall. Both nanoparticles showed better activity against gram negative bacterial compare to gram positive. Hence, the compounds can further used as anti-bacterial agent against highly pathogen gram negative bacteria. Synthesized nanoparticles didn't showed promising anti-fungal activity against C. albicans, therefore further studies are required to confirm the antifungal activity of the bacterial synthesized nanoparticles.

©IJRASET: All Rights are Reserved | SJ Impact Factor 7.538 | ISRA Journal Impact Factor 7.894 |

REFERENCES

[1] Rai M. , Yadav. A, Gade. A. Silver nanoparticles as a new generation of antimicrobials. Biotechnology Advances. 2009; 27: 76.
[2] Leiter H., Nanostructured materials: Basic concepts and microstructures, Act Mater., 2001; 48: 1.
[3] Whitesides G.M, The 'right' size in nanobiotechnology Nat. Biotechnol. 2003; 21:1161.
[4] S. J. P. Jacob, P.R. A. Narayanan and J.S Finub, Green synthesis of silver nanoparticle using Piper nigramleaf extracts and its cytotoxic activity against hep-2 cell line World. J. Pharm. Res. 2013; 2(5):1607.
[5] M. Forough, K. Farhadi, Biological and green synthesis of silver nanoparticles, Turkish J. Eng. Env. Sci. 2010; 34: 281.
[6] M. Sastry, V. Patil, and S.R. Sainkar, Electrostatically controlled diffusion of carboxylic acid derivatized silver colloidal particles in thermally evaporated fatty amine films, J. Phys. Chem. B, 1998; 102: 1404.
[7] N. Dasgupta, B. De, Antioxidant activity of Piper betle L. leaf extract in vitro, Food Chem 2004; 88: 219.
[8] D. Choudhury.., Kale. R.K.,Antioxidant and non-toxic properties of piper betle leaf extract: in vitro and in vivo studies, Phytother Res. 2002; 16: 461.
[9] Annamalai, S.T Babu, N.A Jose, D. Sudha, C.V Lyza. Biosynthesis and characterization of silver and gold nanoparticles using aqueous leaf extraction of Phyllanthus amarus Schum. And Thonn. World Appl Sci J. 2011; 13:1833–1840.
[10] Kumar, X. Zhang, X. J. Liang, Gold nanoparticles: emerging paradigm for targeted drug delivery system, Biotechnol Adv. 2013; 31(5): 593.
[11] Samrot, A. V., Rohan, B., Kumar, D., Sahiti, K., Raji, P., & Samanvitha, S. K. (2016). Detection of antioxidant and antibacterial activity of Mangifera indica using TLC bio-autography.International Journal of Pharmaceutical Sciences and Research,7(11), 4467–4472.
[12] Sahiti, K., Raji, P., Rohan, B., Kumar, D., & Samrot, A. V. (2016). In vitro bioactivity screening of Desmostachya bipinnata. Research Journal of Pharmacy and Technology, 9(4), 361–364.
[13] Amin, M. M., Sawhney, S. S., & Jassal, M. M. S. (2013). Qualitative and quantitative analysis of phytochemicals of Taraxacum officinale. Wudpecker Journal of Pharmacy and Pharmocology, 2(1), 001–005.
[14] Ortega, M. H., Moreno, A. O., Navarro, M. D. H., Cevallos, G. C., Alvarez, L. D., & Mondragon, H. N. (2012). Antioxidant, antinociceptive, and anti-inflammatory effects of carotenoids extracted from dried pepper (Capsicum annuum L.). Journal of Biomedicine and Biotechnology, 524019, 1–10.
[15] Bhutia, K. L., Meetei, N. G. T., & Khanna, V. K. (2016). In vitro regeneration of Dalle khursani, an important chilli cultivar of Sikkim, using various explants. Agrotechnology, 5(1), 142.
[16] Wall, M. M., Waddell, C. A., & Bosland, P. W. (2001). Variation in β-carotene and total carotenoid content in fruits of Capsicum. Hortscience, 36, 746–749.
[17] Breithaupt, D. E., & Schwack, W. (2000). Determination of free and bound carotenoids in paprika (Capsicum annuum L.) by LC/MS. European Food Research and Technology, 211(1), 52–55.
[18] Cervantes-Paz, B., Yahia, E. M., Ornelas-Paz, J. J., VictoriaCampos, C. I., Junquera, I. V., Pérez-Martínez, J. D., &
[19] Escalante-Minakata, P. (2014). Antioxidant activity and content of chlorophylls and carotenoids in raw and heat-processed Jalapeño peppers at intermediate stages of ripening. Food Chemistry, 146,188–196.
[20] Giuffrida, D., Dugo, P., Torre, G., Bignardi, C., Cavazza, A., Corradini, C., & Dugo, G. (2013). Characterization of 12 Capsicum varieties by evaluation of their carotenoid profile and pungency determination. Food Chemistry, 140(4), 794–802.
[21] Richins, R. D., Hernandez, L., Dungan, B., Hambly, S., Holguin, F. O., & O'Connell, M. A. (2010). A Bgreen^ extraction protocol to recover red pigments from hot Capsicum fruit. Hortscience, 45(7),1084–1087.
[22] Bielski, B. H., Richter, H. W., & Chan, P. C. (1975). Some properties of the ascorbate free radical. Annals of the New York Academy of Sciences, 258, 231–237.
[23] Vanderslice, J. T., Higgs, D. J., Hayes, J. M., & Block, G. (1990). Ascorbic acid and dehydroascorbic acid content of foods-as-eaten. Journal of Food Composition and Analysis, 3, 105–118

©IJRASET: All Rights are Reserved | SJ Impact Factor 7.538 | ISRA Journal Impact Factor 7.894 |



10.22214/IJRASET

45.98

IMPACT FACTOR: 7.129

IMPACT FACTOR: 7.429

INTERNATIONAL JOURNAL FOR RESEARCH

IN APPLIED SCIENCE & ENGINEERING TECHNOLOGY

Call : 08813907089 (24*7 Support on Whatsapp)